Since January 2020 Elsevier has created a COVID-19 resource centre with free information in English and Mandarin on the novel coronavirus COVID-19. The COVID-19 resource centre is hosted on Elsevier Connect, the company's public news and information website.

The American Journal of Pathology, Vol. 192, No. 7, July 2022

ELSEVIER

The American Journal of
PATHOLOGY

ajp.amjpathol.org

CARDIOVASCULAR, PULMONARY, AND RENAL PATHOLOGY

Alcohol Increases Lung Angiotensin-Converting Enzyme 2 Expression and Exacerbates Severe Acute Respiratory Syndrome Coronavirus 2 Spike Protein Subunit 1—Induced Acute Lung Injury in K18-hACE2 Transgenic Mice

Pavel A. Solopov,* Ruben M.L. Colunga Biancatelli,* and John D. Catravas*†

From the Frank Reidy Research Center for Bioelectrics, and the School of Medical Diagnostic and Translational Sciences,† College of Health Sciences, Old Dominion University, Norfolk, Virginia*

Accepted for publication March 31, 2022.

Address correspondence to Pavel A. Solopov, D.V.M., Ph.D., Frank Reidy Research Center for Bioelectrics, Old Dominion University, 4111 Monarch Way, Norfolk, VA 23508.
E-mail: psolopov@odu.edu.

During the severe acute respiratory syndrome coronavirus 2 (SARS-CoV-2) pandemic, alcohol consumption increased markedly. Nearly one in four adults reported drinking more alcohol to cope with stress. Chronic alcohol abuse is now recognized as a factor complicating the course of acute respiratory distress syndrome and increasing mortality. To investigate the mechanisms behind this interaction, a combined acute respiratory distress syndrome and chronic alcohol abuse mouse model was developed by intratracheally instilling the subunit 1 (S1) of SARS-CoV-2 spike protein (S1SP) in K18—human angiotensin-converting enzyme 2 (ACE2) transgenic mice that express the human ACE2 receptor for SARS-CoV-2 and were kept on an ethanol diet. Seventy-two hours after S1SP instillation, mice on an ethanol diet showed a strong decrease in body weight, a dramatic increase in white blood cell content of bronchoalveolar lavage fluid, and an augmented cytokine storm, compared with S1SP-treated mice on a control diet. Histologic examination of lung tissue showed abnormal recruitment of immune cells in the alveolar space, abnormal parenchymal architecture, and worsening Ashcroft score in S1SP- and alcohol-treated animals. Along with the activation of proinflammatory biomarkers [NF-κB, STAT3, NLR family pyrin domain-containing protein 3 (NLRP3) inflammasome], lung tissue homogenates from mice on an alcohol diet showed overexpression of ACE2 compared with mice on a control diet. This model could be useful for the development of therapeutic approaches against alcohol-exacerbated coronavirus disease 2019. *(Am J Pathol 2022, 192: 990—1000; https://doi.org/10.1016/j.ajpath.2022.03.012)*

The severe acute respiratory syndrome coronavirus 2 (SARS-CoV-2) outbreak that began in December 2019 and spread rapidly across the globe causes acute lung injury, severe hypoxemia, and multiorgan failure. SARS-CoV-2 infects host cells by targeting the endothelial angiotensin-converting enzyme 2 (ACE2) in the lung, heart, kidney, and gastrointestinal tissues. The pathophysiology of acute respiratory distress syndrome (ARDS) in SARS-CoV-2 infection includes lung perfusion dysregulation and a cytokine storm that causes increased vascular permeability and disease severity.[1] Coronavirus disease 2019 (COVID-19) also can cause psychosocial problems, including increased alcohol consumption and consequent harms.[2] Alcoholic beverage sales in the United States increased greatly immediately after the stay-at-home orders and relaxing of alcohol restrictions associated with the COVID-19 pandemic.[3] An increase in the black marketing of alcohol also has been reported.[4] Alcohol abuse increased so much that some countries even prohibited alcohol sales during the pandemic lockdown.[5] Alcohol consumption is considered an independent factor that increases the incidence of ARDS,

Supported by the Old Dominion University Research Foundation.
Disclosures: None declared.

https://doi.org/10.1016/j.ajpath.2022.03.012

a severe form of acute lung injury with a mortality rate of up to 50%. This translates to tens of thousands of excess deaths in the United States each year from alcohol-associated lung injury, which is comparable with scarring of the liver (ie, cirrhosis) in terms of alcohol-related mortality.[6,7] Furthermore, people who drink heavily are more likely to get pneumonia.[8] Although acute alcohol exposure (<24 hours) favorsanti-inflammatory responses, chronic alcohol consumption favors proinflammatory cytokine release.[9] Notwithstanding that alcohol consumption alone does not cause ARDS, it makes the lungs susceptible to dysfunction induced by pathologies, such as the inflammatory stresses of sepsis, trauma, and so forth.[10] Studies on human monocytes have shown that several pathogens, when combined with chronic ethanol consumption, promote the production of inflammatory cytokines. In the lung, cytokine production is augmented by ethanol, exacerbating respiratory distress syndrome and greatly increasing the expression of transforming growth factor β (TGF-β).[11]

We recently developed an animal model to study acute lung injury caused by subunit 1 (S1) of the SARS-CoV-2 spike protein (S1SP) using K18−human ACE2 (hACE2) transgenic mice.[12] Intratracheal instillation of S1SP induced coronavirus disease 2019 (COVID-19)−like lung and systemic inflammatory responses, including a cytokine storm in bronchoalveolar lavage fluid (BALF) and serum. The current study used this model to investigate how chronic alcohol consumption may worsen the development of COVID-19−like ARDS.

Materials and Methods

Animals and Treatment Groups

All animal studies were approved by the Old Dominion University Institutional Animal Care and Use Committee and adhered to the principles of animal experimentation as published by the American Physiological Society. Healthy male K18-hACE2 transgenic mice (Jackson Laboratories, Bar Harbor, ME), 8 to 10 weeks old, 20 to 25 g body weight, were placed on the Lieber-DeCarli ’82 (Bio-Serv, Flemington, NJ) control liquid diet for 5 days after arrival at the animal facility and then divided randomly into four groups (Figure 1), as follows: i) vehicle (VEH) group: mice continued on a Lieber-DeCarli ’82 control liquid diet for 14 days and then on day 19 were instilled intratracheally (i.t.) with vehicle (sterile saline) at 2 mL/kg body weight; ii) S1SP group: mice on a control diet for 14 days and then on day 19 instilled i.t. with SARS-CoV-2 S1SP at 400 μg/kg at 2 mL/kg body weight; iii) ethanol VEH group: mice transferred to the Lieber-DeCarli ’82 ethanol liquid diet, consisting of 5% to 6% ethanol, for 2 weeks and then on day 19 instilled i.t. with vehicle (sterile saline) at 2 mL/kg body weight; and iv) ethanol S1SP group: mice transferred to the Lieber-DeCarli ’82 ethanol liquid diet for 2 weeks, then on day 19 instilled i.t. with SARS-CoV-2 S1SP at 400 μg/kg at 2 mL/kg body weight. The Lieber-DeCarli liquid diet contains 36% of calories from either ethanol (ethanol diet) or isocaloric maltose dextrin (control diet), 35% of calories from fat, 11% of calories from carbohydrate, and 18% of calories from protein.[13] All animals consumed liquid food *ad libitum* (approximately 20 to 30 mL/day). Treatment with the ethanol diet produces blood alcohol concentrations of approximately 180 mg/dL by day 10.[14] Mice did not receive water during days 5 to 19. Groups 3 and 4 were transferred to the ethanol diet gradually to minimize stress, as follows: days 5 to 7: mixture of one-third ethanol diet and two-thirds control diet; days 8 to 10: mixture of two-thirds ethanol diet and one-third control diet; and days 11 to 22: ethanol diet only. After i.t. instillation on day 19, mice also were given free access to water. All mice were euthanized on day 22 (72 hours after i.t. instillation).

Histology, Lung Injury Scoring, Fibrosis Scoring, and Steatosis Scoring

Immediately after euthanasia, the chest was opened, the mice were placed in an upright position, the lungs were instilled and inflated through the trachea with 10% formaldehyde to a

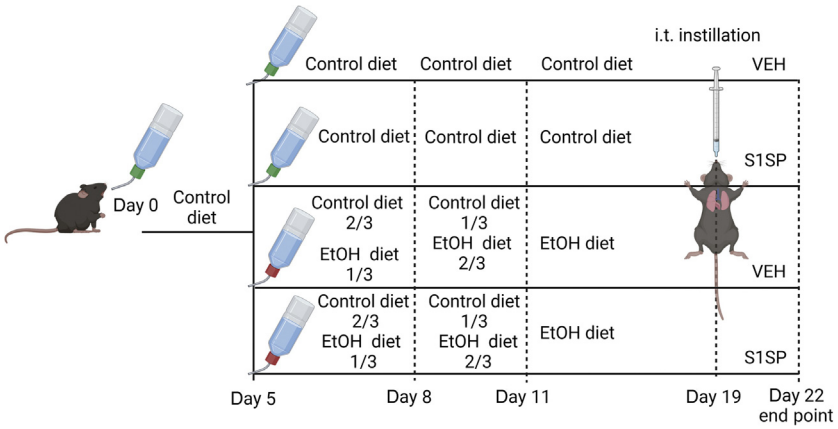

Figure 1 Diagram of experimental design. K18−human angiotensin-converting enzyme 2 transgenic mice received a control or ethanol (EtOH) Lieber-DeCarli ’82 diet for 14 days before the intratracheal (i.t.) instillation of severe acute respiratory syndrome coronavirus 2 or vehicle (saline). Seventy-two hours later, mice were euthanized and lungs, liver, and bronchoalveolar lavage fluid were collected for analysis. $n = 5$/group. VEH, vehicle.

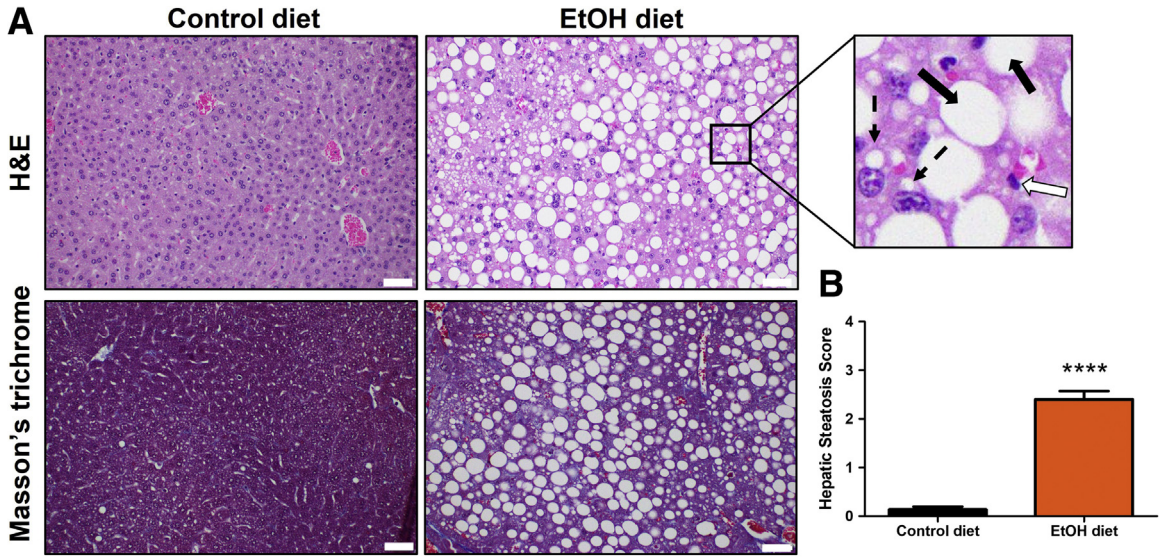

Figure 2 **A:** Histologic analysis [hematoxylin and eosin (H&E) and Masson's trichrome] of the liver on day 19, after 14 days on a control or ethanol (EtOH) Lieber-DeCarli '82 liquid diet. Mice on an alcohol diet show extensive fields of fatty liver: macrovesicular steatosis (**dashed arrow**); large lipid droplets are present in hepatocytes: microvesicular steatosis (**bold arrow**); small lipid droplets are present in hepatocytes: inflammatory cells (**open arrow**). **B:** Hepatic steatosis score. $n = 4$ to 5 mice per group. $^{****}P < 0.0001$ with analysis of variance and the Tukey test. Scale bars = 50 mm. Original magnification, ×20.

pressure of 15 cm H_2O, and then immersed in the same solution. Seventy-two hours later, samples were embedded in paraffin. Sections (5-μm thick) were stained with hematoxylin and eosin (H&E) and Masson's trichrome stains. Twenty randomly selected fields from each slide were examined under immersion (magnification, ×100). Fields from H&E-stained sections were scored according to the Lung Injury Score[15] method to estimate the severity of lung inflammation; this method takes into account histologic evidence of injury, including accumulation of neutrophils in the alveolar or the interstitial space, formation of hyaline membranes, presence of proteinaceous debris in the alveolar space, thickening of the alveolar walls, hemorrhage, and atelectasis. In addition, fields from Masson's trichrome–stained sections were scored according to the Ashcroft score to quantify lung architectural changes and estimate overall collagen deposition.[16]

Livers also were collected and fixed with 10% formaldehyde in the same way and paraffin sections were stained with H&E and Masson's trichrome. Twenty randomly selected fields from each slide were examined. The Hepatic Steatosis Scoring was performed according to the General Nonalcoholic Fatty Liver Disease Scoring System for Rodent Models,[17] which takes into account hepatocellular steatosis, hypertrophy, and inflammation.

BALF White Blood Cell Count

BALF was collected by instilling and withdrawing 1 mL sterile 1× phosphate-buffered saline via the tracheal cannula. The BALF was centrifuged at 2400 × *g* for 10 minutes at 4°C (5417R centrifuge; Thermo Fisher, Waltham, MA) and the supernatant was collected and stored immediately at -80°C. The cell pellet was resuspended in 1 mL sterile phosphate-buffered saline and the total number of white blood cells was determined using a hemocytometer, differential analysis was performed with the Wright-Giemsa stain kit.

All histopathologic and morphologic analyses were performed by an investigator blinded to the study groups (P.A.S.).

Total Protein and Cytokine Analysis in BALF

BALF supernatant was collected and prepared as described in the previous paragraph. Protein concentration was determined using the micro–bicinchoninic acid assay according to the manufacturer's protocol. BALF supernatant IL-6, keratinocyte-derived chemokine (KC), monocyte chemoattractant protein 1 (MCP-1), TGF-β1, and tumor necrosis factor α (TNFα) were analyzed in triplicate via mouse/human enzyme-linked immunosorbent assay kits.

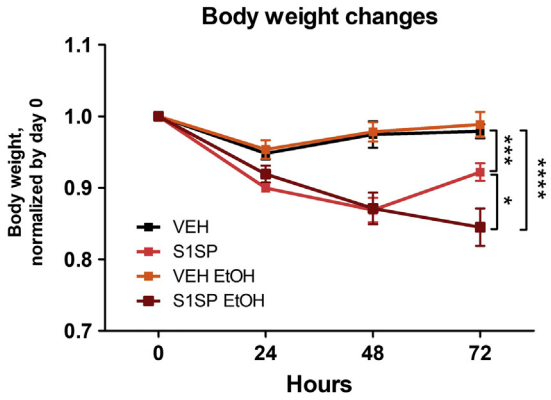

Figure 3 Body weight changes in mice on alcohol (EtOH) or control diets after intratracheal instillation of the severe acute respiratory syndrome coronavirus 2 S1 subunit spike protein (S1SP). $n = 5$ mice per group. $^{*}P < 0.05$, $^{***}P < 0.001$, and $^{****}P < 0.0001$, with analysis of variance and the Tukey test. VEH, vehicle.

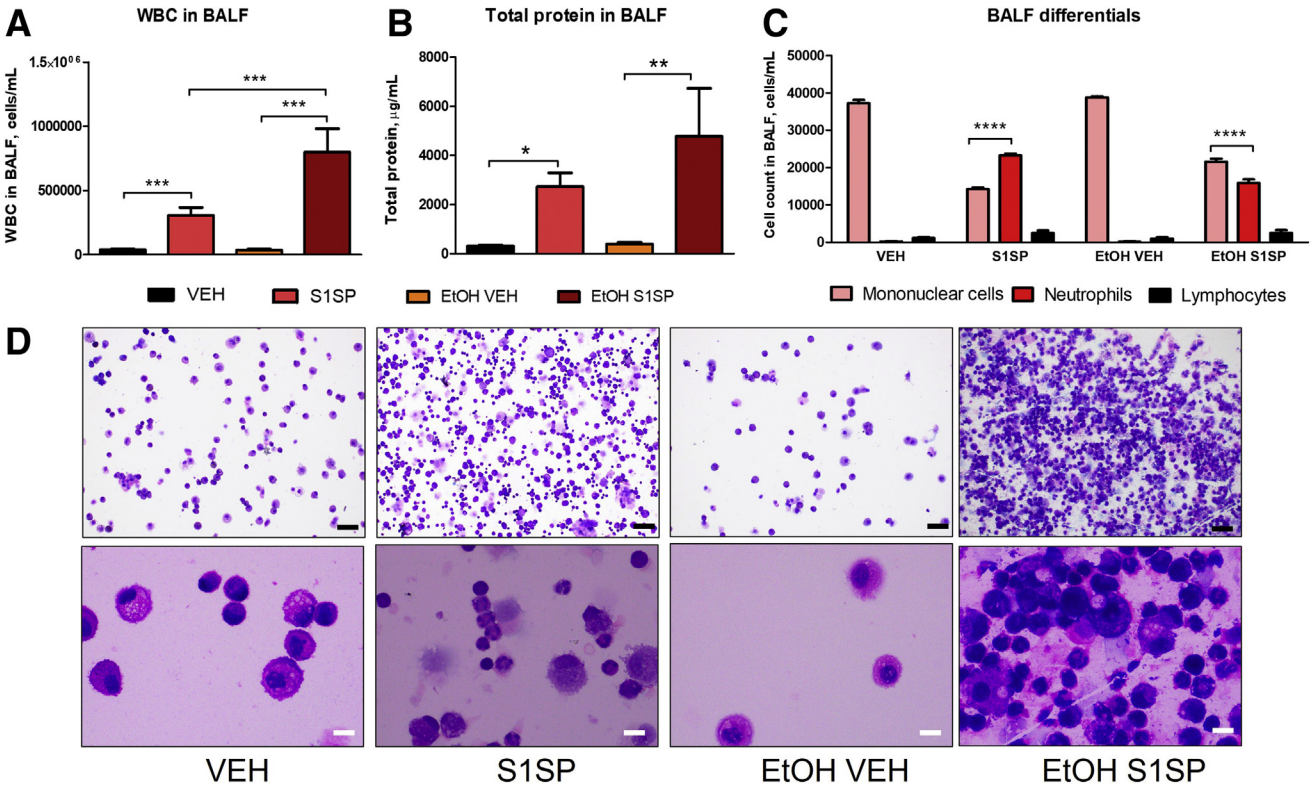

Figure 4 **A**–**D:** White blood cells (WBCs) (**A**), total protein concentration (**B**), and leukocyte differentials (**C** and **D**) in bronchoalveolar lavage fluid (BALF) 72 hours after intratracheal instillation of severe acute respiratory syndrome coronavirus 2 S1 subunit spike protein (S1SP). Means ± SEM. $n = 4$ to 5 per group. $^{*}P < 0.05$, $^{**}P < 0.01$, $^{***}P < 0.001$, and $^{****}P < 0.0001$ with analysis of variance and the Tukey test. Scale bars = 10 mm. Original magnification, ×100. EtOH, alcohol; VEH, vehicle.

Lung Tissue Collection

Immediately after euthanasia, the thorax was opened, blood was drained from the heart through the right ventricle, and the pulmonary circulation was flushed with sterile phosphate-buffered saline containing EDTA. The lungs were dissected from the thorax, snap-frozen in liquid nitrogen, and kept at -80°C for subsequent analysis.

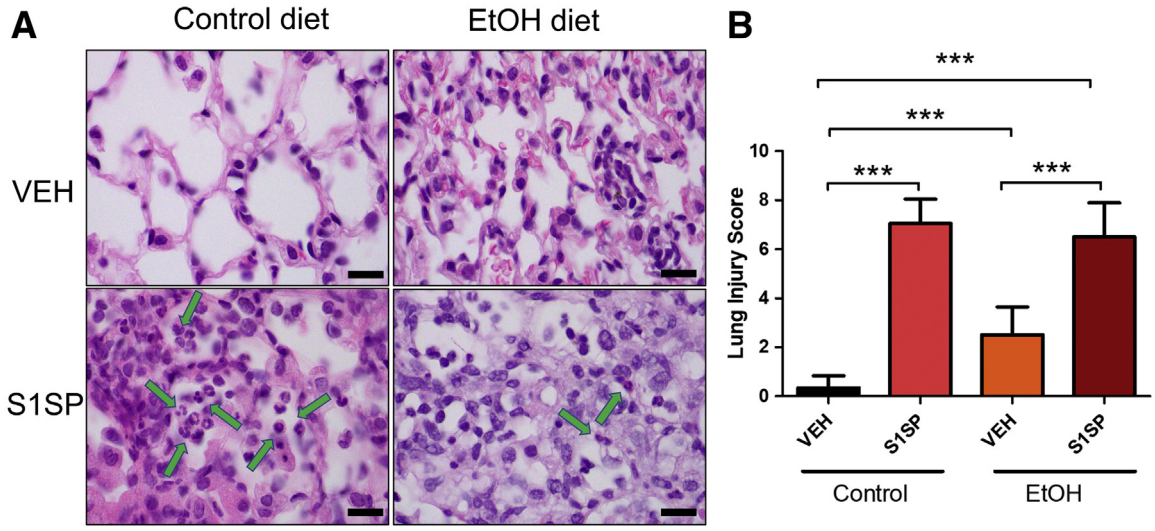

Figure 5 **A** and **B:** H&E staining of lung sections (**A**) and the Lung Injury Score (**B**) from K18–human angiotensin-converting enzyme 2 transgenic mice on normal and alcohol (EtOH) diets 72 hours after intratracheal instillation of either saline or severe acute respiratory syndrome coronavirus 2 S1 subunit spike protein (S1SP). **Green arrows** indicate the recruitment of neutrophils in the alveolar spaces. Means ± SEM. $n = 4$ to 5 per group. $^{***}P < 0.001$ with analysis of variance and the Tukey test. Scale bars = 10 mm. Original magnification, ×100. VEH, vehicle.

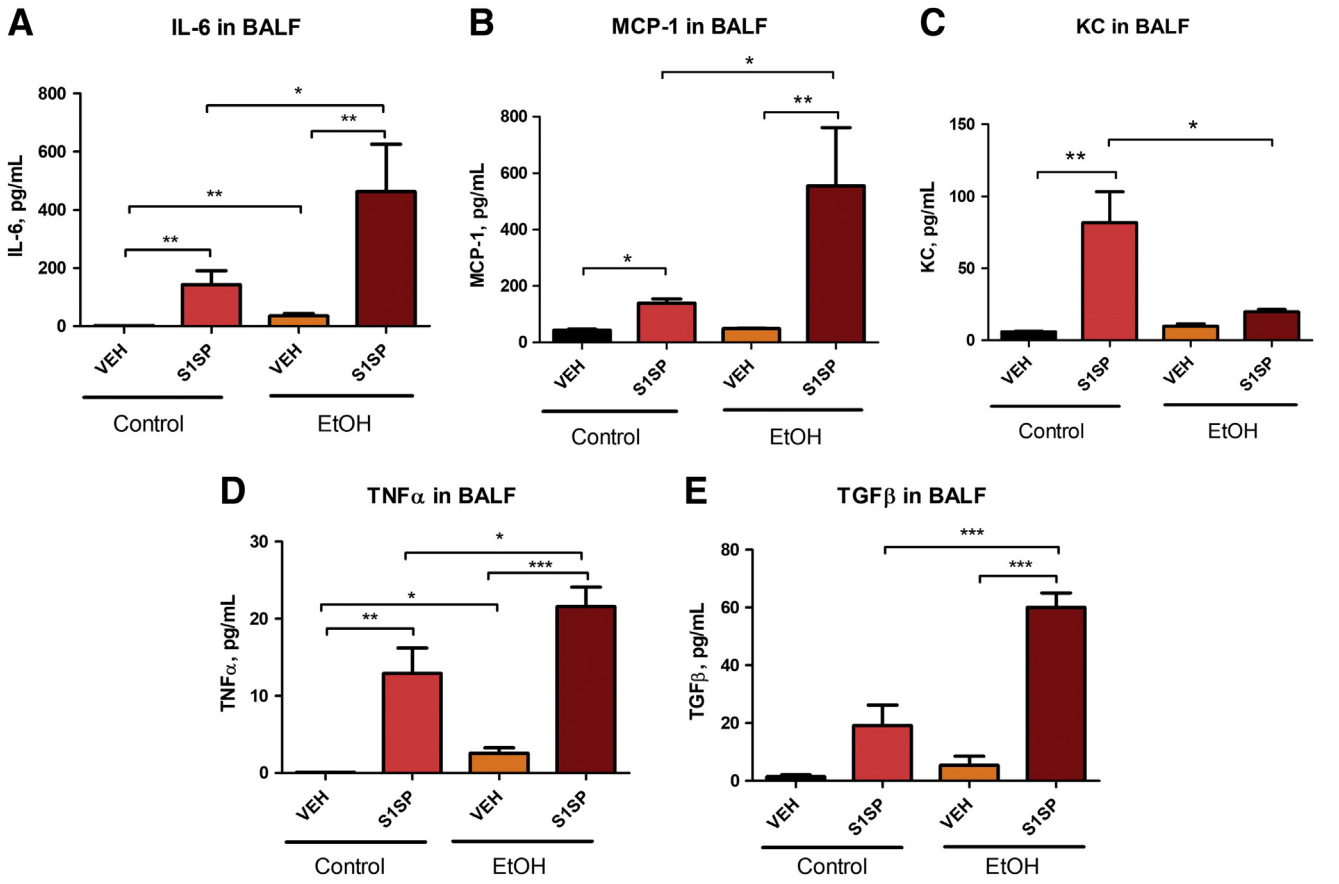

Figure 6 **A**–**E:** Expression levels of inflammatory cytokines IL-6 (**A**), monocyte chemoattractant protein-1 (MCP-1) (**B**), keratinocyte-derived chemokine (KC) (**C**), TNFα (**D**), and TGF-β1 (**E**) in bronchoalveolar lavage fluid (BALF) 72 hours after intratracheal instillation of severe acute respiratory syndrome coronavirus 2 S1 subunit spike protein (S1SP). Means ± SEM. $n = 4$ to 5 per group. $^{*}P < 0.05$, $^{**}P < 0.01$, and $^{***}P < 0.001$ with analysis of variance and the Tukey test. EtOH, alcohol; VEH, vehicle.

Western Blot Analysis

Proteins in lung tissue homogenates were extracted from frozen lungs by ultrasonic homogenization (50% amplitude, 3 times, 10 seconds each time) in ice-cold lysing radioimmunoprecipitation assay buffer with added protease inhibitor cocktail (100:1). The protein lysates were gently mixed under rotation for 3 hours at 4°C, and then centrifuged twice at 14,000 × *g* for 10 minutes at 4°C. The supernatants were collected, and the total protein concentration was analyzed using the micro–bicinchoninic acid assay. Equal amounts of proteins from all samples (1000 μg/mL) were used for Western blot analysis. The lysates were first mixed with tricine sample buffer 1:1, boiled for 5 minutes, and then separated on a 10% polyacrylamide SDS gel by electrophoresis. Separated proteins then were transferred to a nitrocellulose membrane, incubated overnight at 4°C with the appropriate primary antibody, diluted in the blocking buffer, followed by a 1-hour incubation with the secondary antibody at room temperature, and scanned by digital fluorescence imaging (Odyssey CLx; LI-COR, Dallas, TX). β-actin was used as loading control. ImageJ software version 1.8.0 (NIH, Bethesda, MD; *http://imagej.nih.gov/ij*, last accessed July 18, 2021) was used to perform densitometry of the bands from the Western blot membranes. Some membranes were stripped for 5 minutes and incubated with other primary and secondary antibodies.

RNA Isolation and Quantitative Real-Time PCR

Lung tissue, stored in RNAlater solution (Thermo Fisher) for at least 24 hours, was dried and homogenized in TRIzol, followed by a cleaning step using the RNeasy Mini Kit. The purified RNA was transcribed into cDNA using the SuperScript IV VILO Reverse Transcription Kit and analyzed by real-time quantitative PCR with SYBR Green Master Mix on a StepOne Real-Time PCR System (version 2.3; Applied Biosystems, San Francisco, CA). Results were evaluated using the standard curve method and expressed as fold of control values. β-actin mRNA expression was used for the normalization of all samples.

Statistical Analysis

Statistical significance of differences among groups was determined by one-way or two-way analysis of variance followed by the Tukey *post hoc* test using GraphPad Prism

Software (GraphPad Software, San Diego, CA). Differences among groups were considered significant at $P < 0.05$.

Results

To make sure that 14 days of ethanol diet is sufficient for the development of chronic alcohol abuse symptoms, morphologic changes in liver samples were observed by H&E and Masson's trichrome staining. K18-hACE2 transgenic mice on 14 days of an alcohol diet were investigated. Prominent signs of severe fatty liver disease (steatosis) (Figure 2A) reflected in the profoundly increased hepatic steatosis score (Figure 2B) were seen. Mice on a control diet showed healthy liver architecture.

Alcohol consumption had no effect on the body weight of transgenic mice instilled with saline. A decrease in appetite after anesthesia was reflected in a slight weight loss during the first 24 hours. Unlike control mice, both groups of transgenic mice instilled with S1SP showed a rapid decrease in body weight. However, mice on a control diet started to recover 48 hours after instillation, while alcohol-consuming animals continued to lose weight (Figure 3).

Mice on a regular diet instilled with S1SP showed a significant increase in leukocyte content of BALF compared with the VEH group. Mice on an alcohol diet and treated with S1SP showed a dramatic increase in the white blood cell content of BALF compared with S1SP-instilled mice on a normal diet (Figure 4A). There was no difference between control and ethanol diets in the two VEH groups. A similar profile also was observed in the total protein levels in BALF, suggesting exacerbated capillary permeability and further confirming the presence of strong acute inflammation (Figure 4B). A BALF white blood cell differential analysis showed an upward shift of mononuclear cell content in ethanol-fed, S1SP-instilled mice, while neutrophils primarily increased in S1SP-instilled mice on a control diet (Figure 4, C and D).

H&E-stained lung sections from mice on a control diet instilled with S1SP showed recruitment of neutrophils and a higher lung injury score than vehicle-instilled mice on a control diet. Mice on an ethanol diet and instilled with saline showed a higher number of interstitial mononuclear cells compared with mice on a control diet, altered parenchymal architecture, and a higher lung injury score (Figure 5). S1SP-instilled mice on an ethanol diet showed mononuclear cell infiltration with minimal interstitial neutrophils, abnormal alveolar structure, and a lung injury score (calculated as per the Official American Thoracic Society Workshop Report[15]) that was threefold higher than mice on a control diet.

IL-6 and TNFα concentrations in BALF increased in the VEH-instilled group on an alcohol diet compared with the normal diet VEH group (Figure 6). Both S1SP-instilled groups showed increased levels of IL-6 and TNFα compared with their respective controls. However, S1SP-instilled mice on an ethanol diet showed even higher values of both cytokines. Similar results were observed with TGF-β1. Similar to other cytokines, MCP-1 was increased in the ethanol S1SP group. However, significant up-regulation of KC was observed in S1SP-treated mice on a control diet only, in agreement with histologic and BALF neutrophil concentration data that depicted much lower lung and BALF neutrophil presence in ethanol-S1SP–treated mice (Figure 6).

To explore the potential effect of increased TGF-β levels on fibroblast activation, fixed lung sections were additionally stained with Masson's trichrome to visualize collagen deposition. Significant changes in parenchymal architecture, including thickening of the alveolar walls as well as multiple

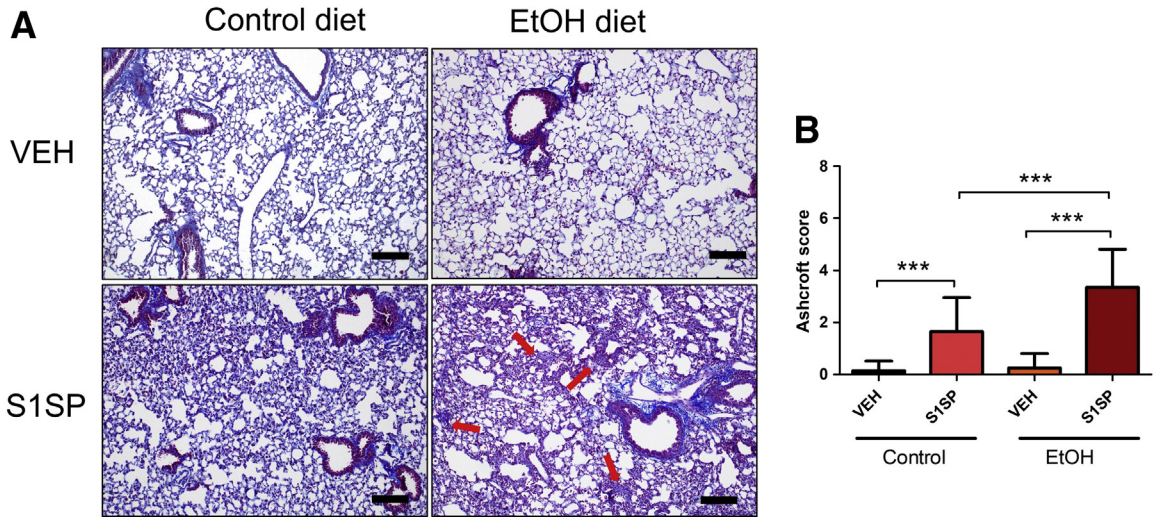

Figure 7 **A** and **B:** Masson's trichrome staining of lung sections (**A**) and the Ashcroft score (**B**) from K18–human angiotensin-converting enzyme 2 transgenic mice on normal and alcohol (EtOH) diets 72 hours after intratracheal instillation of either saline or severe acute respiratory syndrome coronavirus 2 S1 subunit spike protein (S1SP). **Red arrows** indicate the deposition of collagen in the alveolar spaces. Means ± SEM. $n = 4$ to 5 per group. ***$P < 0.001$ with analysis of variance and the Tukey test. Scale bars = 50 mm. Original magnification, ×20. VEH, vehicle.

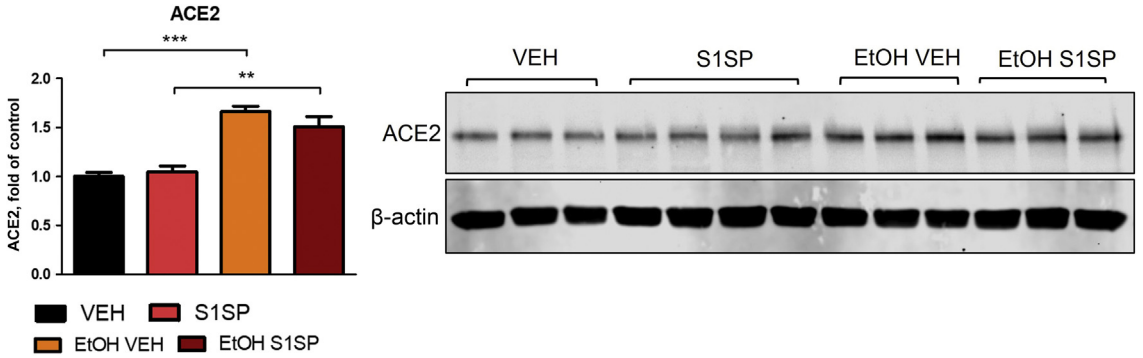

Figure 8 K18—human angiotensin-converting enzyme 2 (ACE2) transgenic mice on an alcohol (EtOH) diet instilled with the S1 subunit spike protein (S1SP) show overexpression of ACE2 in lung tissue homogenates. Means ± SEM. $n = 3$ to 4. $^{**}P < 0.01$, $^{***}P < 0.001$ with analysis of variance and the Tukey test. VEH, vehicle.

segments with significant collagen deposition, were observed in S1SP-instilled mice that received alcohol (Figure 7).

Lung tissue homogenates from mice on an alcohol diet showed overexpression of ACE2 compared with mice on a control diet. S1SP did not affect ACE2 expression further (Figure 8).

Intratracheal instillation of a single element of SARS-CoV-2, S1SP, into K18-hACE2 transgenic mice increase the expression of proinflammatory biomarkers in the lung.[12] This was confirmed in the current study, in which Western blot analysis of lung homogenates showed significant increases in the phosphorylation of both STAT3 and nuclear factor of kappa light polypeptide gene enhancer in B-cells inhibitor (IkBα) in transgenic mice on a control diet instilled with S1SP. Alcohol significantly amplified the inflammatory effect of S1SP. Moreover, S1SP significantly increased the expression of inflammasome NLRP3, and even more so in mice on an ethanol diet (Figure 9). Profound activation of both extracellular signal-regulated kinase and protein kinase

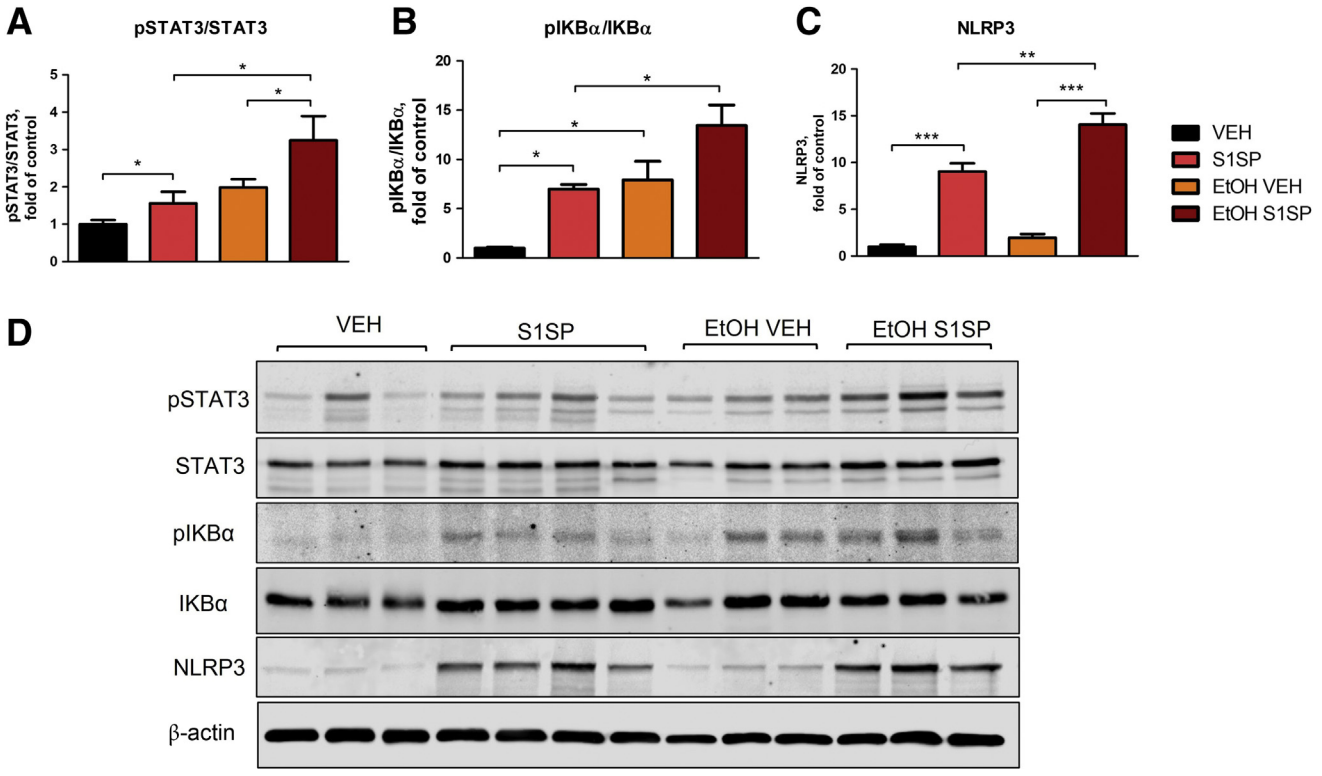

Figure 9 **A** and **B:** K18—human angiotensin-converting enzyme 2 transgenic mice on an alcohol (EtOH) diet instilled with S1 subunit spike protein (S1SP) show activation of STAT3 (**A**) and nuclear factor of kappa light polypeptide gene enhancer in B-cells inhibitor (IkBα) (**B**) in lung tissue homogenates. **C:** S1SP also increased inflammasome NLRP3 expression, especially in mice on an ethanol diet. **D:** Western blot analysis; protein band density was normalized to that of β-actin. For IkBα and STAT3, the ratio of phosphorylated to total was calculated and all three are presented as fold of control (VEH). Means ± SEM. $n = 3$ to 4. $^{*}P < 0.05$, $^{**}P < 0.01$, and $^{***}P < 0.001$ with analysis of variance and the Tukey test. pIkBα, phospho-IkBα; pSTAT3, phospho-STAT3; VEH, vehicle.

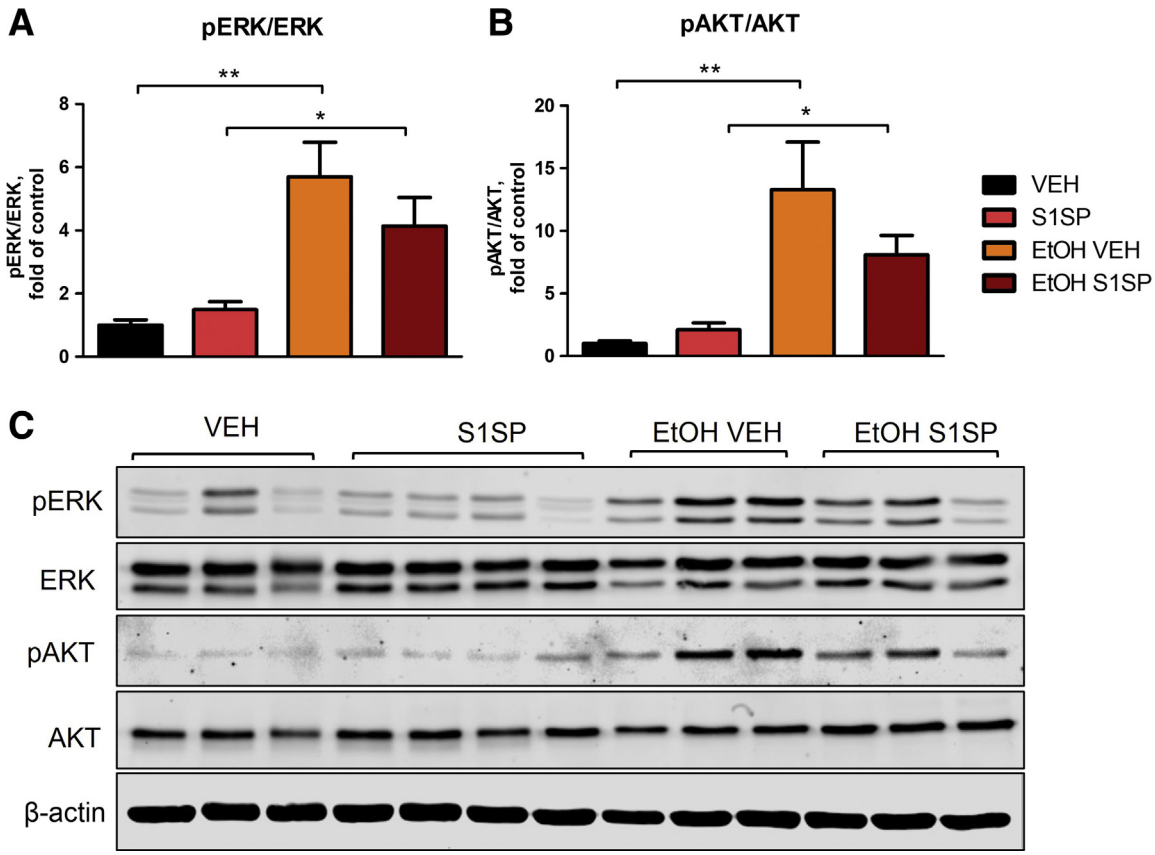

Figure 10 **A** and **B:** K18—human angiotensin-converting enzyme 2 transgenic mice on an alcohol (EtOH) diet instilled with either vehicle or S1SP show increased phosphorylation of extracellular signal-regulated kinase (ERK) (**A**) and protein kinase B (AKT) (**B**) in lung tissue homogenates. Western blot analysis; protein band density was normalized to that of β-actin. **C:** The ratio of phosphorylated to total was calculated and presented as fold of control (VEH). Means ± SEM. $n = 3$ to 4. $^{*}P < 0.05$, $^{**}P < 0.01$ with analysis of variance and the Tukey test. pAKT, phospho-AKT; pERK, phospho-ERK; S1SP, S1 subunit spike protein; VEH, vehicle.

B (AKT) signaling was observed in mice on an alcohol diet. This occurred in both VEH- and S1SP-instilled groups (Figure 10).

Discussion

A novel mouse model of SARS-CoV-2 in combination with an established model of chronic and binge ethanol feeding [the National Institute on Alcohol Abuse and Alcoholism (NIAAA) model[18]] was used to study the exacerbations of ARDS induced by SARS-CoV-2 S1SP *in vivo*, thereby simulating the pathogenesis of COVID-19 disease in alcoholics.

The NIAAA model is widely recognized and useful for the study of alcoholic liver disease and systemic damage by alcohol consumption. This model is similar to the drinking pattern in patients with alcoholic hepatitis, who have a background of chronic alcoholism and a record of recent excessive alcohol consumption in anamnesis.[18] The model suggests using 8- to 10-week-old male C57BL/6 mice because they are an alcohol-preferring strain and have shown the best survival rate. Other strains either refuse the alcohol diet or are affected too adversely by the 5% ethanol and, as a consequence, they lose weight and have high mortality rates.[19] Oral ethanol gavage (binge) was not used so as to avoid the possibility of compounded distress from ethanol and acute lung injury. However, mice in the present study showed damaged livers, as reflected in profound steatosis. As described previously in more detail, the SARS-CoV-2 S1SP at 400 μg/kg body weight i.t. was used to induce a COVID-19—like acute lung injury.[12] Similar to the previous study, transgenic mice on a normal diet instilled with S1SP showed a decrease in body weight that began recovering 48 hours later. However, in alcohol-exposed mice, S1SP produced a continuously decreasing body weight, in agreement with a recent study in which loss of body weight was significantly higher in alcohol-treated mice infected with *Aspergillus fumigatus* compared with similarly infected mice that did not receive alcohol.[20] This also agrees with the observation that heavy alcohol drinkers are at risk for abnormal long-term weight loss.[21]

Severe alveolar inflammation is one of the basic characteristics of ARDS associated with COVID-19. After endothelial barrier dysfunction,[22] a large number of leukocytes

and plasma proteins are released into the alveolar space. S1SP could be a key factor to increasing lung vascular permeability during COVID-19.[12] The activation of the proinflammatory transcription factors IKBα, STAT3, and NLRP3 inflammasome in the lung are likely important mediators. All of these inflammatory mechanisms are enhanced by alcohol consumption. Ethanol has been reported to independently cause hyperactivation of STAT3, IKBα, and NLRP3 inflammasome both *in vitro* and *in vivo*.[23–25]

Monocyte, macrophage, and especially neutrophil recruitment were observed in the BALF, and alveolar space of mice instilled with S1SP. In intensive care units, COVID-19 patients present excessive alveolar infiltration of neutrophils.[26] Neutrophil recruitment to the focus of infection is fundamental for the fight against the invading pathogens.[27] Chronic alcohol ingestion disturbs both immunologic and nonimmunologic host defense mechanisms within the airway.[28] Neutrophil recruitment into the airways is reduced in alcohol-exposed mice infected with *A. fumigatus*.[20] Importantly, no pathohistologic differences between alcoholic and nonalcoholic groups were observed in the first 2 days after infection. This was corroborated by predominantly mononuclear cell recruitment in alveoli of alcohol-treated mice receiving S1SP, in contrast to S1SP-instilled mice on a normal diet who showed primarily neutrophil infiltration. At the same time, spike protein–altered lung parenchymal structure was not significantly different between mice on control and ethanol diets. Monocytes and macrophages play an important role in the pathogenesis of both alcoholic liver disease[29] and acute lung injury.[30] These cells, infected via ACE2-independent and ACE2-dependent pathways, lose their ability to fight the virus and induce adaptive immune responses.[31,32] Their impaired functions can lead to multiple organ damage, mainly owing to exacerbation of acute lung injury, provocation of a cytokine storm, and development of fibrosis.[33] Patient BALF analysis has shown that alcohol causes alveolar macrophage dysfunction and an alcohol-induced increase in oxidative stress.[34,35] Herein, hyperexpression of ACE2 in lung

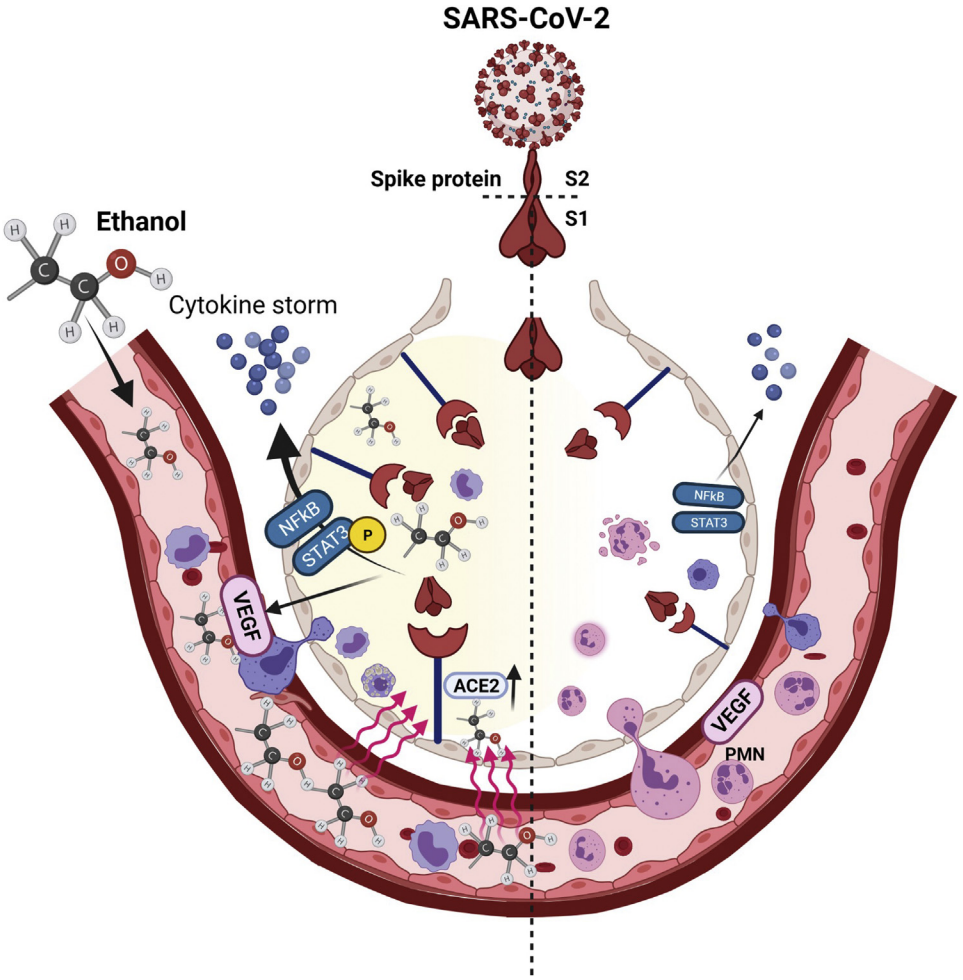

Figure 11 Signaling pathways in severe acute respiratory syndrome coronavirus 2 (SARS-CoV-2) S1 subunit spike protein (S1SP)– (**right**) and alcohol-exacerbated SARS-CoV-2 S1SP–induced acute lung injury (**left**). ACE2, angiotensin-converting enzyme 2; PMN, polymorphonuclear leukocytes; VEGF, vascular endothelial growth factor.

homogenates of K18-hACE2 transgenic mice on an alcohol diet was observed, suggesting an additional mechanism of exacerbation of COVID-19 by ethanol.

Additional evidence of worsening of COVID-19–related ARDS by alcohol consumption is provided by the dramatic increase of cytokine concentration in BALF. Compared with controls, mice instilled with S1SP show overexpression of cytokines, in agreement with previous data.[12] Herein, even saline-instilled mice on an ethanol diet showed significant increases in IL-6 and TNFα compared with control mice. A few clinical studies have indicated anti-inflammatory properties of alcohol, including a reduction in IL-6, while animal studies have suggested a linear relationship between alcohol drinking and IL-6.[36] Ethanol consumption alters both IL-6 and TNFα expression in lipopolysaccharide-challenged Kupffer cells.[37] Similarly, modest alcohol consumption suppresses TNFα levels in monocytes, probably by suppressing post-transcriptional TNFα production. However, mice who received daily 2.5 g/kg ethanol by gavage for 4 days (acute model) showed increased TNFα and decreased NF-κB activity in plasma, thus unleashing the apoptotic effects of TNFα.[38] Herein, the cytokine storm, associated with COVID-19–like ARDS, is more pronounced in alcohol-consuming animals. A recent meta-analysis of gene expression profiles in COVID-19 patients predicted that ethanol may augment systemic inflammation by enhancing the activity of IL-1β, IL-6, and TNF.[39] The lack of KC activation in BALF taken from S1SP mice on an alcohol diet compared with S1SP mice on a control diet is consistent with the observed monocyte/neutrophil shift in BALF. This finding suggests that chronic alcohol consumption may change the immune response in ARDS. The activation of TGF-β is critical to the development of pulmonary edema in acute lung injury and also plays an important role in the development of pulmonary fibrosis.[30,40–42] The expression of TGF-β1, CD44v6, matrix metallopeptidase 9 (MMP-9), caveolin-1, and other tissue biomarkers of the TGF-β signaling pathway, along with the deposition of extracellular matrix components, collagen I, collagen III, and α-smooth muscle actin, has been detected in lung sections from COVID-19 patients.[43] In the present model, alcohol did not increase the expression of TGF-β1 in mice instilled with saline, but amplified it in S1SP-instilled animals.

The SARS-CoV-2 spike protein leads to the induction of transcriptional regulatory molecules, such as NF-κB and mitogen-activated protein kinase/extracellular signal-regulated kinase (MAPK) 42/44.[44] Activation of mitogen-activated protein kinase by COVID-19 plays an important role in the survival of the virus.[45] Modulation of the mitogen-activated protein kinase pathway by alcohol is variable and depends on the organ, cell type, and acute or chronic exposure, but its mechanism has been poorly studied in lungs.[46] SARS-CoV-2 endocytosis occurs through a clathrin-mediated pathway, regulated by phosphatidylinositol 3-kinase (PI3K)/AKT signaling. The AKT signaling pathway was activated by the N protein of SARS-CoV in Vero E6 cells.[47] Activation of the AKT also has been linked to the induction of lung fibrosis in patients with COVID-19. The current study showed a dramatic activation of extracellular signal-regulated kinase 42/44 and AKT, which may, in part, explain the associated pathologies.

In summary, the current data show that K18-hACE2 transgenic mice on an alcohol diet exhibit a more severe S1SP-induced ARDS than corresponding mice on a control diet, and that overexpression of ACE2 may play a critical role in this process (Figure 11). How alcohol consumption will affect the lungs in the late stages of COVID-19 is not clear, especially considering that the proinflammatory pathways studied here also are involved in the development of pulmonary fibrosis. Thus, this model could be useful for the development of therapeutic interventions against alcohol-exacerbated COVID-19.

References

1. Cai A, McClafferty B, Benson J, Ramgobin D, Kalayanamitra R, Shahid Z, Groff A, Aggarwal CS, Patel R, Polimera H, Vunnam R, Golamari R, Sahu N, Bhatt D, Jain R: COVID-19: catastrophic cause of acute lung injury. S D Med 2020, 73:252–260
2. Pfefferbaum B, North CS: Mental health and the Covid-19 pandemic. N Engl J Med 2020, 383:510–512
3. Grossman ER, Benjamin-Neelon SE, Sonnenschein S: Alcohol consumption during the COVID-19 pandemic: a cross-sectional survey of US adults. Int J Environ Res Public Health 2020, 17:9189
4. Nadkarni A, Kapoor A, Pathare S: COVID-19 and forced alcohol abstinence in India: the dilemmas around ethics and rights. Int J Law Psychiatry 2020, 71:101579
5. Pedrosa AL, Bitencourt L, Fróes ACF, Cazumbá MLB, Campos RGB, de Brito SBCS, Simões E Silva AC: Emotional, behavioral, and psychological impact of the COVID-19 pandemic. Front Psychol 2020, 11:566212
6. Kershaw CD, Guidot DM: Alcoholic lung disease. Alcohol Res Health 2008, 31:66–75
7. Thakur L, Kojicic M, Thakur SJ, Pieper MS, Kashyap R, Trillo-Alvarez CA, Javier F, Cartin-Ceba R, Gajic O: Alcohol consumption and development of acute respiratory distress syndrome: a population-based study. Int J Environ Res Public Health 2009, 6:2426–2435
8. Samokhvalov AV, Irving HM, Rehm J: Alcohol consumption as a risk factor for pneumonia: a systematic review and meta-analysis. Epidemiol Infect 2010, 138:1789–1795
9. Barr T, Helms C, Grant K, Messaoudi I: Opposing effects of alcohol on the immune system. Prog Neuropsychopharmacol Biol Psychiatry 2016, 65:242–251
10. Guidot DM, Hart MC: Alcohol abuse and acute lung injury: epidemiology and pathophysiology of a recently recognized association. J Investig Med 2005, 53:235
11. Crews FT, Bechara R, Brown LA, Guidot DM, Mandrekar P, Oak S, Qin L, Szabo G, Wheeler M, Zou J: Cytokines and alcohol. Alcohol Clin Exp Res 2006, 30:720–730
12. Colunga Biancatelli R, Solopov P, Sharlow ER, Lazo JS, Marik PE, Catravas JD: The SARS-CoV-2 spike protein subunit 1 induces COVID-19-like acute lung injury in K18-hACE2 transgenic mice and barrier dysfunction in human endothelial cells. Am J Physiol Lung Cell Mol Physiol 2021, 321:L477–L484
13. Dong Y, Qiu P, Zhao L, Zhang P, Huang X, Li C, Chai K, Shou D: Metabolomics study of the hepatoprotective effect of Phellinus igniarius in chronic ethanol-induced liver injury mice using UPLC-

Q/TOF-MS combined with ingenuity pathway analysis. Phytomedicine 2020, 74:152697
14. Ghosh Dastidar S, Warner JB, Warner DR, McClain CJ, Kirpich IA: Rodent models of alcoholic liver disease: role of binge ethanol administration. Biomolecules 2018, 8:3
15. Matute-Bello G, Downey G, Moore BB, Groshong SD, Matthay MA, Slutsky AS, Kuebler WM; Acute Lung Injury in Animals Study Group: An official American Thoracic Society workshop report: features and measurements of experimental acute lung injury in animals. Am J Respir Cell Mol Biol 2011, 44(5):725−738
16. Ashcroft T, Simpson JM, Timbrell V: Simple method of estimating severity of pulmonary fibrosis on a numerical scale. J Clin Pathol 1988, 41:467−470
17. Liang W, Menke AL, Driessen A, Koek GH, Lindeman JH, Stoop R, Havekes LM, Kleemann R, van den Hoek AM: Establishment of a general NAFLD scoring system for rodent models and comparison to human liver pathology. PLoS One 2014, 9:e115922
18. Bertola A, Mathews S, Ki SH, Wang H, Gao B: Mouse model of chronic and binge ethanol feeding (the NIAAA model). Nat Protoc 2013, 8:627−637
19. Wei VL, Singh SM: Genetically determined response of hepatic aldehyde dehydrogenase activity to ethanol exposures may be associated with alcohol sensitivity in mouse genotypes. Alcohol Clin Exp Res 1988, 12:39−45
20. Malacco NLSdO, Souza JAM, Martins FRB, Rachid MA, Simplicio JA, Tirapelli CR, Sabino AdP, Queiroz-Junior CM, Goes GR, Vieira LQ, Souza DG, Pinho V, Teixeira MM, Soriani FM: Chronic ethanol consumption compromises neutrophil function in acute pulmonary Aspergillus fumigatus infection. Elife 2020, 9:e58855
21. Chao AM, Wadden TA, Tronieri JS, Berkowitz RI: Alcohol intake and weight loss during intensive lifestyle intervention for adults with overweight or obesity and diabetes. Obesity (Silver Spring) 2019, 27:30−40
22. Roberts KA, Colley L, Agbaedeng TA, Ellison-Hughes GM, Ross MD: Vascular manifestations of COVID-19 − thromboembolism and microvascular dysfunction. Front Cardiovasc Med 2020, 7:598400
23. Narayanan PD, Nandabalan SK, Baddireddi LS: Role of STAT3 phosphorylation in ethanol-mediated proliferation of breast cancer cells. J Breast Cancer 2016, 19:122−132
24. Nennig SE, Schank JR: The role of NFkB in drug addiction: beyond inflammation. Alcohol Alcohol 2017, 52:172−179
25. Priyanka SH, Thushara AJ, Rauf AA, Indira M: Alcohol induced NLRP3 inflammasome activation in the brain of rats is attenuated by ATRA supplementation. Brain Behav Immun Health 2020, 2:100024
26. Pandolfi L, Fossali T, Frangipane V, Bozzini S, Morosini M, D'Amato M, Lettieri S, Urtis M, Di Toro A, Saracino L, Percivalle E, Tomaselli S, Cavagna L, Cova E, Mojoli F, Bergomi P, Ottolina D, Lilleri D, Corsico AG, Arbustini E, Colombo R, Meloni F: Bronchoalveolar inflammation in COVID-19 patients: a correlation with clinical outcome. BMC Pulm Med 2020, 20:301
27. Kolaczkowska E, Kubes P: Neutrophil recruitment and function in health and inflammation. Nat Rev Immunol 2013, 13:159−175
28. Simou E, Leonardi-Bee J, Britton J: The effect of alcohol consumption on the risk of ARDS: a systematic review and meta-analysis. Chest 2018, 154:58−68
29. McClain CJ, Hill DB, Song Z, Deaciuc I, Barve S: Monocyte activation in alcoholic liver disease. Alcohol 2002, 27:53−61
30. Pittet JF, Griffiths MJ, Geiser T, Kaminski N, Dalton SL, Huang X, Brown LA, Gotwals PJ, Koteliansky VE, Matthay MA, Sheppard D: TGF-beta is a critical mediator of acute lung injury. J Clin Invest 2001, 107:1537−1544
31. McKechnie JL, Blish CA: The innate immune system: fighting on the front lines or fanning the flames of COVID-19? Cell Host Microbe 2020, 27:863−869
32. Schulte-Schrepping J, Reusch N, Paclik D, Baßler K, Schlickeiser S, Zhang B, et al: Severe COVID-19 is marked by a dysregulated myeloid cell compartment. Cell 2020, 182:1419−1440.e23
33. Meidaninikjeh S, Sabouni N, Marzouni HZ, Bengar S, Khalili A, Jafari R: Monocytes and macrophages in COVID-19: friends and foes. Life Sci 2021, 269:119010
34. Brown LA, Ping XD, Harris FL, Gauthier TW: Glutathione availability modulates alveolar macrophage function in the chronic ethanol-fed rat. Am J Physiol Lung Cell Mol Physiol 2007, 292:L824−L832
35. Yeh MY, Burnham EL, Moss M, Brown LAS: Chronic alcoholism alters systemic and pulmonary glutathione redox status. Am J Respir Crit Care Med 2007, 176:270−276
36. Dai J, Lin D, Zhang J, Habib P, Smith P, Murtha J, Fu Z, Yao Z, Qi Y, Keller ET: Chronic alcohol ingestion induces osteoclastogenesis and bone loss through IL-6 in mice. J Clin Invest 2000, 106:887−895
37. Marasliogl M, Oppermann E, Blattner C, Weber R, Henrich D, Jobin C, Schleucher E, Marzi I, Lehnert M: Chronic ethanol feeding modulates inflammatory mediators, activation of nuclear factor-κB, and responsiveness to endotoxin in murine Kupffer cells and circulating leukocytes. Mediators Inflamm 2014, 2014:808695
38. Robin MA, Demeilliers C, Sutton A, Paradis V, Maisonneuve C, Dubois S, Poirel O, Lettéron P, Pessayre D, Fromenty B: Alcohol increases tumor necrosis factor alpha and decreases nuclear factor-kappab to activate hepatic apoptosis in genetically obese mice. Hepatology 2005, 42:1280−1290
39. Huang W, Zhou H, Hodgkinson C, Montero A, Goldman D, Chang SL: Network meta-analysis on the mechanisms underlying alcohol augmentation of COVID-19 pathologies. Alcohol Clin Exp Res 2021, 45:675−688
40. Solopov P, Colunga Biancatelli RM, Dimitropoulou C, Catravas JD: Dietary phytoestrogens ameliorate hydrochloric acid-induced chronic lung injury and pulmonary fibrosis in mice. Nutrients 2021, 13:3599
41. Yue X, Shan B, Lasky JA: TGF-β: titan of lung fibrogenesis. Curr Enzym Inhib 2010, 6. 10.2174/10067
42. Solopov P, Marinova M, Dimitropoulou C, Colunga Biancatelli RML, Catravas JD: Development of chronic lung injury and pulmonary fibrosis in mice following acute exposure to nitrogen mustard. Inhal Toxicol 2020, 32:141−154
43. Vaz de Paula CB, Nagashima S, Liberalesso V, Collete M, da Silva FP, Oricil AG, Barbosa GS, da Silva GV, Wiedmer DB, da Silva Dezidério F, Noronha L: COVID-19: immunohistochemical analysis of TGF-β signaling pathways in pulmonary fibrosis. Int J Mol Sci 2022, 23:168
44. Patra T, Meyer K, Geerling L, Isbell TS, Hoft DF, Brien J, Pinto AK, Ray RB, Ray R: SARS-CoV-2 spike protein promotes IL-6 trans-signaling by activation of angiotensin II receptor signaling in epithelial cells. PLoS Pathog 2020, 16:e1009128
45. Ghasemnejad-Berenji M, Pashapour S: SARS-CoV-2 and the possible role of Raf/MEK/ERK pathway in viral survival: is this a potential therapeutic strategy for COVID-19? Pharmacology 2021, 106:119−122
46. Aroor AR, Shukla SD: MAP kinase signaling in diverse effects of ethanol. Life Sci 2004, 74:2339−2364
47. Mizutani T, Fukushi S, Ishii K, Sasaki Y, Kenri T, Saijo M, Kanaji Y, Shirota K, Kurane I, Morikawa S: Mechanisms of establishment of persistent SARS-CoV-infected cells. Biochem Biophys Res Commun 2006, 347:261−265